Postprint of: Kozieł S., Pietrenko-Dąbrowska A., Expedited Acquisition of Database Designs for Reduced-Cost Performance-Driven Modeling and Rapid Dimension Scaling of Antenna Structures, IEEE TRANSACTIONS ON ANTENNAS AND PROPAGATION (2021), pp. 1-13,
https://ieeexplore.ieee.org/document/9416865

Expedited Acquisition of Database Designs for Reduced-Cost Performance-Driven Modeling and Rapid Dimension Scaling of Antenna Structures

Slawomir Koziel, *Senior Member*, *IEEE*, and Anna Pietrenko-Dabrowska, *Senior Member*, *IEEE*

***Abstract*—Fast replacement models have been playing an increasing role in high-frequency electronics, including the design of antenna structures. Their role is to improve computational efficiency of the procedures that normally entail large numbers of expensive full-wave electromagnetic (EM) simulations, e.g., parametric optimization or uncertainty quantification. Recently introduced performance-driven modeling methods, such as the nested kriging framework, alleviate some of the common difficulties pertinent to conventional modeling methods. These include the curse of dimensionality but also the need for rendering models to be valid for broad ranges of antenna parameters and operating conditions, as dictated by the design utility of the surrogates. The keystone of performance-driven methods is an appropriate confinement of the model domain so that the training data is only acquired in the regions containing high-quality designs. Identification of such regions is realized using a set of so-called reference designs pre-optimized for selected ensembles of performance requirements. The CPU cost of generating the reference points may be considerable and compromise the savings obtained by operating in a constrained domain. In this paper, a technique for automated, reliable and low-cost acquisition of the reference designs is proposed. Our methodology involves inverse sensitivities, iterative correction procedures, and accelerated feature-based gradient search with sparse Jacobian updates. It is validated using three microstrip antenna examples and demonstrated as an efficient tool for lowering the cost of building surrogate models within the nested kriging framework. The intended use of our approach is expedited construction of database designs for constrained modeling frameworks, construction of inverse surrogates as well as procedures for rapid re-design and dimension scaling of antenna structures.**

***Index Terms*— Antenna design; design optimization; surrogate modeling; EM-driven design; performance-driven modeling.**

I. Introduction

The importance of fast surrogate models in the development and design automation of modern antenna structures has been gradually increasing over the recent years [1]-[5]. Their primary role is to replace computationally expensive full-wave electromagnetic (EM) simulations when conducting procedures that require massive analyses of the structure at hand, in particular, parameter tuning [6], [7], statistical analysis [8]-[10], multi-objective design [11]-[13], or tolerance-aware optimization [14], [15]. Among the two basic classes of surrogate models, the data-driven ones are by far the most popular due to their versatility and accessibility (e.g., through various toolboxes [16], [17], implemented in high-level programming environments such as Matlab [18]). Widely used techniques of this group include polynomial regression [19], kriging interpolation [20], radial basis functions [21], artificial neural networks [22], support vector regression [23], or polynomial chaos expansion [24].

Data-driven models are obtained using sampled simulation data and are typically fast to evaluate. However, their construction is hindered by the curse of dimensionality [25], i.e., a rapid growth of the number of training data samples necessary to achieve the assumed accuracy, but also a related problem, which is that usable models need to be valid over broad ranges of the system parameters. Acquisition of the training data over a large parameter space incurs considerable CPU expenses, which may be prohibitive if the model domain dimensionality becomes excessive. High nonlinearity of antenna responses only aggravates the problem. Several techniques were developed to mitigate these problems, including high-dimensional model representation (HDMR) [26], orthogonal matching pursuit (OMP) [27], least-angle regression (LAR) [28], or variable-fidelity methods (co-kriging [29], two-stage Gaussian process regression [30], Bayesian model fusion [31], etc.).

The second class of surrogates are physics-based models, normally constructed by correcting the underlying low-fidelity models (e.g., equivalent networks or coarse-discretization EM simulations). These models are relatively immune to the dimensionality issues; however, they rarely exhibit universal approximation properties [32], their evaluation cost may be considerable [33], and their versatility is limited because the low-fidelity models are problem-specific [34]. Consequently, physics-based surrogates are mostly employed for local optimization purposes [35]. The popular techniques include space mapping [36], response correction methods (e.g., manifold mapping [37], adaptive response scaling [38]), or feature-based optimization [39].

The manuscript was submitted on July 7, 2020. This work was supported in part by the Icelandic Centre for Research (RANNIS) Grant 206606051, and by National Science Centre of Poland Grant 2017/27/B/ST7/00563.

S. Koziel is with Engineering Optimization and Modeling Center of Reykjavik University, Reykjavik, Iceland (e-mail: koziel@ru.is); A. Pietrenko-Dabrowska and also S. Koziel are with Faculty of Electronics, Telecommunications and Informatics, Gdansk University of Technology, 80-233 Gdansk, Poland.

Recently, the concept and implementation of performance-driven modelling has been proposed [40], [41], where the issues related to the curse of dimensionality and wide ranges of parameters to be covered by the model are addressed by appropriate confinement of the model domain. As opposed to a conventional approach, where the surrogate is set up in a domain defined by the lower/upper bounds for the system parameters, the performance-driven methods seek for a region containing designs that are optimum or nearly optimum with respect to the performance figures relevant to the antenna structure at hand. The volume of such a region is significantly smaller than that of the interval-type of domain and focusing the modelling process therein allows for rendering reliable models using small numbers of training data samples and without formally restricting the ranges of the antenna parameters. Several variations of the performance-driven modelling methods have been proposed [40]-[45], with a notable example of the nested kriging framework [45], capable of handling arbitrary number of performance figures and allowing straightforward design of experiments and surrogate model optimization.

The surrogate model domain in the performance-driven frameworks is defined using a set of reference designs, pre-optimized for selected target vectors of the figures of interest (e.g., the antenna operating frequencies or permittivity values of the substrate the antenna is to be implemented on). These designs may be available from the prior design work with the same antenna structure but in some cases they have to be generated from scratch, which is a computationally expensive process, adding up to the overall cost of setting up the surrogate model. Furthermore, acquisition of the reference designs is difficult to automate because the optimization process has to be carried out over broad ranges of the target values of the figures of interest. A certain reduction of the number of reference designs can be achieved by using sensitivity data as demonstrated in [46] using gradient-enhanced kriging [47]. Notwithstanding, the problem remains because optimizing the antenna for significantly altered operating conditions is a non-trivial task, which often requires incorporation of a certain amount of experience even to generate reasonable starting points (e.g., through parameter sweeping). It should also be mentioned that the sets of pre-optimized designs play important roles in setting up inverse surrogates (e.g., [48]-[51]), as well as in numerical procedures for expedited parameter tuning [52]. Consequently, the development of reliable algorithms for automated and fast rendering the databases of optimized antenna designs is of a practical necessity.

This paper proposes an algorithmic framework for low cost, reliable, and automated generation of antenna reference designs corresponding to the predefined target values of performance figures. Our approach involves an inverse surrogate model, which is constructed at the level of response features, and identified using sensitivities of the optimized antenna geometry parameters with respect to the figures of interest. The surrogate is used to yield a starting point for further tuning, realized by means of trust-region gradient search with Broyden-based Jacobian updates. Reliability of the optimization process is ensured by design specifications adaptation, which is launched if the initial design is not of sufficient quality or if direct optimization fails. The presented technique is demonstrated using several antenna structures with the databases of sizes up to ten designs rendered at the costs of less than a few dozen (up to 30 or 40) of EM simulations per design. For comparison, the cost of creating the same databases using traditional approach (direct optimization occasionally aided by parameter sweeping to improve the starting points) is significantly higher, around a hundred EM simulations per design on the average. Application examples for performance-driven modeling and rapid re-design of antennas are also provided along with the analysis of the benefits enabled by the proposed methodology. The originality and the technical contributions of this work include: (i) the development of the novel algorithmic framework for low-cost acquisition of database designs for a variety of applications such as surrogate modeling, inverse modeling, or rapid dimension scaling, (ii) increasing reliability of the antenna parameter adjustment processes and reducing the need for the designer interaction (e.g., through supervised parameter sweeping), (iii) implementing a framework for design automation and antenna optimization within broad ranges of the operating conditions. All of these are of practical importance due to addressing some common challenges of EM-driven procedures, which are both imperative and ubiquitous in the design of modern antennas.

II. Database Designs: Problem Statement. Objective Space, Response Features and Inverse Sensitivity

This section states the problem considered in the paper, i.e., the acquisition of a set of antenna designs, optimized for selected target values of performance figures of interest. We also introduce the necessary notation, in particular, the concept of the objective space. Some additional algorithmic components are also discussed, to be used in Section III, specifically, the response features and feature-based assessment of design quality, as well as the inverse sensitivity (the gradients of the optimum antenna geometry parameters with respect to the figures of interest) and its estimation method.

A. Objective Space and Design Optimality. Problem Statement

Let $\boldsymbol{x} = [x_1 \ldots x_n]^T$ be the vector of designable parameters of the antenna structure under design. Typically, x_k are the antenna dimensions. The parameter space X is defined as an interval $[\boldsymbol{l}\ \boldsymbol{u}]$, where $\boldsymbol{l} = [l_1 \ldots l_n]^T$ and $u = [u_1 \ldots u_n]^T$ are the lower and upper bounds for the parameters, so that we have $l_k \le x_k \le u_k$, $k = 1, \ldots, n$.

Consider the performance figures F_k, $k = 1, \ldots, N$, and the objective vector $\boldsymbol{F} = [F_1 \ldots F_N]^T$. The figures F_k might be the intended operating frequencies of a multi-band antenna, the target bandwidth, but also the material parameters, e.g., the relative permittivity of the substrate the antenna is to be implemented on. The objective space F is defined using the lower bounds $\boldsymbol{l}_F = [l_{F.1} \ldots l_{F.N}]^T$ and upper bounds $\boldsymbol{u}_F = [u_{F.1} \ldots u_{F.N}]^T$ for F_k, so that $\boldsymbol{F} \in F$ if and only if $\boldsymbol{l}_F \le \boldsymbol{F} \le \boldsymbol{u}_F$ (inequalities understood component-wise).

Given the target vector $\boldsymbol{F}$, the design problem is to find

$$\boldsymbol{x}^* = U^*(\boldsymbol{F}) = \arg\min_x U(\boldsymbol{x}, \boldsymbol{F}) \quad (1)$$

where U is a scalar merit function to be minimized. The function U is related to the performance figures F_k, and its particular formulation depends on the problem. Let us consider a few examples that clarify the above concepts and notation.

- *Example 1*. Suppose that the goal is to improve the matching of a multi-band antenna at the intended operating frequencies $f_{0.k}$, k = 1, …, N. In this case, the performance figures will be $F_k = f_{0.k}$, and the merit function can be defined as

$$U(\boldsymbol{x},\boldsymbol{F}) = \max\{|S_{11}(\boldsymbol{x},F_1)|,...,|S_{11}(\boldsymbol{x},F_N)|\} \quad (2)$$

- *Example 2*. Consider a circular polarization antenna that is supposed to operate at the center frequency f_0 with a fractional bandwidth B (symmetric w.r.t. f_0) so that the antenna is well matched in that bandwidth (i.e., $|S_{11}| \le -10$ dB over B) and the axial ratio $AR \le 3$ dB over B. Assuming that B is fixed and the goal is to design the antenna for a specific frequency f_0, the only performance figure would be $F_1 = f_0$, and the merit function may be defined as

$$U(\boldsymbol{x},\boldsymbol{F}) = \max_{F_1\left(1-\frac{B}{2}\right)\le f\le F_1\left(1+\frac{B}{2}\right)} AR(\boldsymbol{x},f) + \beta c(\boldsymbol{x})^2 \quad (3)$$

where

$$c(\boldsymbol{x}) = \max_{F_1\left(1-\frac{B}{2}\right)\le f\le F_1\left(1+\frac{B}{2}\right)} \left\{\frac{|S_{11}(\boldsymbol{x},f)|+10}{10}, 0\right\} \quad (4)$$

Here, minimization of the axial ratio over the required bandwidth (centered at f_0) is the primary objective, whereas the matching condition is controlled using the penalty term $\beta c(\boldsymbol{x})$ (β being a positive penalty factor) that quantifies a possible violation of the condition $|S_{11}| \le -10$ dB.

- *Example 3*. Consider the antenna to be designed for the center frequency f_0, so that the fractional impedance bandwidth is at least B (symmetric w.r.t. f_0), and the average realized gain is maximized within the same bandwidth. Assuming that both the center frequency and the bandwidth are to be optimizable goals, the performance figures are $F_1 = f_0$ and $F_2 = B$. The merit function could be defined as

$$U(\boldsymbol{x},\boldsymbol{F}) = -(F_1F_2)^{-1}\int_{F_1(1-F_2/2)}^{F_1(1+F_2/2)} G(\boldsymbol{x},f)df + \beta c(\boldsymbol{x}) \quad (5)$$

where, $G(\boldsymbol{x},f)$ is the realized gain (as a function of the parameter vector $\boldsymbol{x}$) at the frequency f, whereas $\beta c(\boldsymbol{x})$ is a penalty term, similar to that used in Example 2.

- *Example 4*. Consider a UWB antenna operating in the frequency range 3.1 GHz to 10.6 GHz. The goal is to reduce the antenna footprint $A(\boldsymbol{x})$ while ensuring $|S_{11}| \le -10$ dB within the UWB frequency range. The antenna is to be implemented on the substrate of permittivity ε_r and the height h, both being parts of the objective space (i.e., the antenna is to be designed to minimize its footprint for a specific dielectric substrate within a prescribed ranges of permittivity and height). Thus, we have $F_1 = \varepsilon_r$, $F_2 = h$, and the merit function is defined as

$$U(\boldsymbol{x},\boldsymbol{F}) = A(\boldsymbol{x}) + \beta c([\boldsymbol{x}^T\ \boldsymbol{F}^T]^T) \quad (6)$$

where $\beta c(\boldsymbol{x})$ is a penalty term, similar to that used in Example 2 but this time it is a function of the objective vector $\boldsymbol{F} = [F_1\ F_2]^T = [\varepsilon_r\ h]^T$ because the antenna reflection also depends on the substrate parameters.

B. Response Features. Feature-Based Design Quality Assessment

The response feature technology [39], [53] allows us to explore a specific structure of the antenna responses (e.g., the presence of resonances) to reduce the computational cost of the optimization and modelling procedures. This comes from an observation that the coordinates of appropriately defined feature points depend in a less nonlinear manner on the geometry parameters of the structure than the original outputs (typically, frequency characteristics). Consequently, it might be beneficial to re-define the design problem from the original, e.g., minimax formulation, to that involving the response features [39]. Furthermore, feature-based formulation often makes local optimization routines sufficient in situations where the conventional problem statement would call for a globalized search [54].

To clarify this, let us consider an example of a multi-band antenna to be optimized in the sense of (2) (Section II.*B*). Typically, the feature points of the input characteristic would be related to the location of the antenna resonances as well as the frequencies corresponding to –10 dB levels of $|S_{11}|$ (e.g., for the purpose of bandwidth manipulation), see Fig. 1. In general, the vector of antenna feature points will be denoted as $\boldsymbol{p}(\boldsymbol{x}) = [p_1(\boldsymbol{x})\ \ldots\ p_L(\boldsymbol{x})]^T$. In our example, the locations of the resonances are sufficient for reformulating the problem (2), specifically, their frequencies $f_{r.k}$ and levels $l_{r.k}$, k = 1, …, N. These will be used as the response features. Thus, the feature vector can be written as $\boldsymbol{p}(\boldsymbol{x}) = [f_{r.1}(\boldsymbol{x})\ \ldots\ f_{r.N}(\boldsymbol{x})\ l_{r.1}(\boldsymbol{x})\ \ldots\ l_{r.N}(\boldsymbol{x})]^T$. The problem (2) can be then reformulated using the feature-based objective function U_F as

$$U_F(\boldsymbol{x},\boldsymbol{F}) = \max\{l_{r.1}(\boldsymbol{x}),...,l_{r.N}(\boldsymbol{x})\} + \beta\left\|\begin{bmatrix}F_1\\ \vdots\\ F_N\end{bmatrix} - \begin{bmatrix}f_{r.1}(\boldsymbol{x})\\ \vdots\\ f_{r.N}(\boldsymbol{x})\end{bmatrix}\right\|^2 \quad (7)$$

The optimum design according to (2) is the same as that according to (7). However, the functional landscape of $U_F(\cdot)$ is much more regular than that of $U(\cdot)$ and solving (7) generally requires less computational effort than solving (2). This is illustrated in Fig. 2 using an example of a dual-band antenna.

In practice, generating the database designs for various objective vectors $\boldsymbol{F}$ requires re-design of the antenna for various operating frequencies. Regardless of additional specifications that need to be satisfied (e.g., maximization of gain or bandwidth), allocating the operating frequency (or frequencies) at the target values is the primary goal. This is because handling other antenna characteristics (e.g., improving the matching) is normally easier after the operating band is properly allocated.

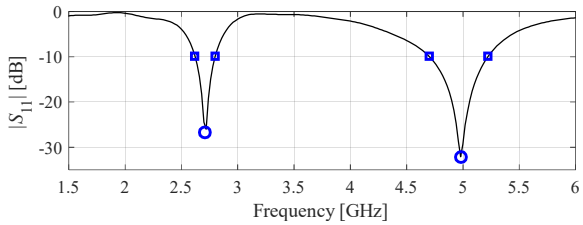

Fig. 1. Response features shown for the example of a dual-band antenna: exemplary reflection characteristic (—), feature points corresponding to the antenna resonances (o), feature points corresponding to –10 dB levels (□).

Z

The optimization framework proposed in this work employs a so-called assessment function $f_a(\boldsymbol{x},\boldsymbol{F}) = f_a(\boldsymbol{p}(\boldsymbol{x}),\boldsymbol{F})$, defined using the response features, which is to serve this particular purpose, i.e., to evaluate the distance between the actual and target objective vector of the antenna at hand.

The function is defined individually for each case; for the sake of clarity, let us consider a few examples:

- *Example 1*: (cf. Example 1 of Section II.*A*) Assume that the goal is to improve the matching of a multi-band antenna at the intended operating frequencies $f_{0.k}$, $k = 1, \ldots, N$. The performance figures will be $F_k = f_{0.k}$, and the response features are $\boldsymbol{p}(\boldsymbol{x}) = [f_{r.1}(\boldsymbol{x}) \ \ldots \ f_{r.N}(\boldsymbol{x}) \ l_{r.1}(\boldsymbol{x}) \ \ldots \ l_{r.N}(\boldsymbol{x})]^T$, where $f_{r.j}$ and $l_{r.j}$ are the frequency and level of the jth resonance. We will denote as $\boldsymbol{F}_{extr}(\boldsymbol{x}) = [f_{r.1}(\boldsymbol{x}) \ \ldots \ f_{r.N}(\boldsymbol{x})]^T$ the actual (extracted from the EM response) objective vector at the design $\boldsymbol{x}$. The assessment function will be then defined as

$$f_a(\boldsymbol{x},\boldsymbol{F}) = \left\|\boldsymbol{F} - \boldsymbol{F}_{extr}(\boldsymbol{x})\right\| = \left\| \begin{bmatrix} F_1 \\ \vdots \\ F_N \end{bmatrix} - \begin{bmatrix} f_{r.1}(\boldsymbol{x}) \\ \vdots \\ f_{r.N}(\boldsymbol{x}) \end{bmatrix} \right\|^2 \tag{8}$$

- *Example 2*: (cf. Example 3 of Section II.*A*) Consider the antenna to be designed for the center frequency f_0, so that the fractional impedance bandwidth is at least B, and the average realized gain is maximized within the same bandwidth. The performance figures are $F_1 = f_0$ and $F_2 = B$. For the purpose of defining the assessment function, we consider the feature points corresponding to the antenna resonance (f_r and l_r) and the –10 dB points determining the antenna bandwidth ($f_{L.j}$ and $l_{L.j}$, $j = 1, 2$). If, at a particular design $\boldsymbol{x}$, we have $l_r > -10$ dB, we assign $f_{L.j} = f_r$ and $l_{L.j} = l_r$. Using these, the assessment function can be defined as

$$f_a(\boldsymbol{x},\boldsymbol{F}) = \left| F_1 - \frac{f_{L.1} + f_r + f_{L.2}}{3} \right| \tag{9}$$

  In this case, $\boldsymbol{F}_{extr} = [(f_{L.1} + f_r + f_{L.2})/3 \ B]$. In general, the assessment function can be defined as $f_a(\boldsymbol{x},\boldsymbol{F}) = \|\boldsymbol{F} - \boldsymbol{F}_{extr}\|$, with $\boldsymbol{F}_{extr}$ set up to make this definition consistent with particular definitions (here, (8) and (9)).

C. Inverse Sensitivity and Its Estimation

The next component of the proposed optimization framework is the inverse sensitivity, i.e., $\boldsymbol{J}^x(\boldsymbol{F}) = \partial\boldsymbol{x}/\partial\boldsymbol{F} = \partial U^*(\boldsymbol{F})/\partial\boldsymbol{F}$. The entries J_{jk}^x of the Jacobian $\boldsymbol{J}^x(\boldsymbol{F})$ are the partial derivatives of the (optimized) antenna parameters x_j with respect to the performance figures F_k.

The problem is that these derivatives are not available directly and cannot be computed using finite differentiation. Below, we provide a simple procedure for their estimation which is partially analytical, and partially relies on optimization.

We will denote by $\boldsymbol{J}(\boldsymbol{x})$ the Jacobian matrix of the EM antenna model $\boldsymbol{R}$ at the design $\boldsymbol{x}$,. We will also denote as $\boldsymbol{d} = [d_1 \ \ldots \ d_N]^T$ a vector of perturbations of the performance figures. At the first step, we find the perturbed reference designs $\boldsymbol{x}^{(k)}$ corresponding to vectors $[F_1 \ \ldots \ F_k + d_k \ \ldots \ F_N]^T$

$$\boldsymbol{x}^{(k)} = \arg\min_{\boldsymbol{x}} U(\boldsymbol{x},[F_1 \ \ldots F_k + d_k \ F_N]^T) \tag{10}$$

The initial approximation $\boldsymbol{x}^{(k.0)}$ of $\boldsymbol{x}^{(k)}$ will be obtained using the first-order Taylor expansion $\boldsymbol{R}_L$ of the EM model $\boldsymbol{R}$

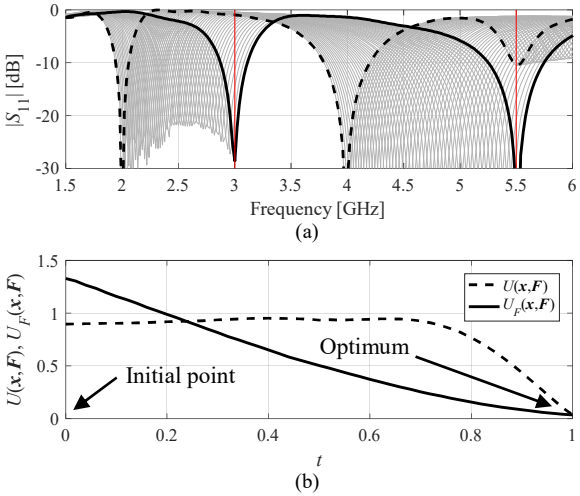

Fig. 2. Conceptual illustration of the benefits of feature-based versus minimax formulation of the parameter tuning problem: (a) initial design (thick dashed line), design optimized for target frequencies 3.0 GHz and 5.5 GHz (thick solid line), and the family of antenna characteristics along the line segment connecting these two designs parameterized by $0 \le t \le 1$ (thin solid lines); (b) minimax objective function (2) (- - -) and feature-based objective function (7) (—) versus parameter t. Note that the feature-based objective function is more regular, and the target design can be reached from the given initial point through local search routine, which is not the case for the minimax formulation.

$$\boldsymbol{R}_L(\boldsymbol{y}) = \boldsymbol{R}(\boldsymbol{x}) + \boldsymbol{J}(\boldsymbol{x})\cdot(\boldsymbol{y} - \boldsymbol{x}) \tag{11}$$

specifically, by minimizing $U(\boldsymbol{x},[F_1 \ \ldots F_k + d_k \ F_N]^T)$ calculated from $\boldsymbol{R}_L$, in the vicinity of $\boldsymbol{x}$. Given $\boldsymbol{x}^{(k.0)}$, the design is then refined using a conventional trust region algorithm

$$\boldsymbol{x}^{(k.i)} = \arg\min_{\boldsymbol{x}, \|\boldsymbol{x} - \boldsymbol{x}^{(k.i-1)}\| \le \delta^{(i)}} U_L^{(i)}(\boldsymbol{x},[F_1 \ \ldots F_k + d_k \ F_N]^T) \tag{12}$$

where $\boldsymbol{x}^{(k.i)}$ is the series of approximations to $\boldsymbol{x}^{(k)}$, and $\delta^{(i)}$ is the trust-region radius adjusted adaptively using the standard trust-region rules [55]. The objective function $U_L^{(i)}$ is defined using the linear model of the form of (11) with the Jacobian matrix updated in each iteration using the rank-one Broyden formula [56]. Using these mechanisms, the computational cost of generating the perturbations $\boldsymbol{x}^{(k)}$ can be kept low, typically at the level of $2n$ EM antenna simulations, where n is the number of independent parameters of the antenna.

Let $[F_1^{(k)} \ \ldots \ F_N^{(k)}]^T$ be the actual values of the performance figures corresponding to $\boldsymbol{x}^{(k)}$, extracted from $\boldsymbol{R}(\boldsymbol{x}^{(k)})$. As the perturbations d_k are small, we have

$$x_l^{(k)} \approx x_l + \sum_{r=1}^{N} J_{lr}^x(\boldsymbol{x})[F_r^{(k)} - F_r] \tag{13}$$

which can be rewritten in the matrix form as

$$\boldsymbol{X} = \boldsymbol{J}^x \boldsymbol{A}_F \tag{14}$$

where

$$\boldsymbol{X} = \left[\boldsymbol{x}^{(1)} - \boldsymbol{x} \ \cdots \ \boldsymbol{x}^{(N)} - \boldsymbol{x}\right] \tag{15}$$

and

$$\boldsymbol{A}_F = \begin{bmatrix} F_1^{(1)} - F_1 & \cdots & F_1^{(N)} - F_1 \\ \vdots & \ddots & \vdots \\ F_N^{(1)} - F_N & \cdots & F_N^{(N)} - F_N \end{bmatrix} \tag{16}$$

The matrix $\boldsymbol{A}_F$ is nonsingular because its diagonal elements are dominant over the off-diagonal entries by construction of the perturbed designs. Thus, (15) can be solved analytically as

This article has been accepted for publication in a future issue of this journal, but has not been fully edited. Content may change prior to final publication. Citation information: DOI 10.1109/TAP.2021.3074632, IEEE Transactions on Antennas and Propagation

$$\boldsymbol{J}^x = \boldsymbol{X}\boldsymbol{A}_F^{-1} \tag{17}$$

The Jacobian $\boldsymbol{J}^x$ will be used to generate an initial approximation of the database designs as explained in Section III.

III. Algorithmic Framework for Low-Cost Database Design Acquisition

This section formulates the proposed framework for database design acquisition. It involves the components described in Section II. The presentation is divided into several parts. In Section III.*A*, we discuss the use of the inverse surrogate to generate the initial designs. Section III.*B* formulates the parameter tuning procedure, whereas Section III.*C* outlines the entire framework, which is then summarized using the flow diagram. Numerical verification of the procedure will be provided in Section IV along with the application examples for performance-driven surrogate modelling of antenna components.

A. Inverse Surrogate. Generating Initial Designs

Let $\boldsymbol{F}^{(k)} \in F$, $k = 1, \ldots, p$, be the set of objective vectors that determine the design database to be acquired, denoted as $\boldsymbol{x}_F^{(k)} = U^*(\boldsymbol{F}^{(k)})$ (cf. (1)). Without loss of generality, we may assume that $\boldsymbol{F}^{(1)}$ is the vector closest to the center of gravity of the set $\{\boldsymbol{F}^{(k)}\}$, i.e., $\boldsymbol{F}_c = p^{-1}\sum_k \boldsymbol{F}^{(k)}$. The first design $\boldsymbol{x}_F^{(1)} = U^*(\boldsymbol{F}^{(1)})$ is obtained using direct search, e.g., through feature-based optimization [39] to reduce the computational cost of the process. Using this design as well as the inverse sensitivity $\boldsymbol{J}^x(\boldsymbol{F}^{(1)})$ found as described in Section II.*C*, we set up a linear (inverse) surrogate of the form

$$\boldsymbol{s}(\boldsymbol{F}) = \boldsymbol{x}_F^{(1)} + \boldsymbol{J}^x(\boldsymbol{F}^{(1)})\cdot(\boldsymbol{F} - \boldsymbol{F}^{(1)}) \tag{18}$$

The initial design $\boldsymbol{x}_F^{(k.0)}$ for finding the database design $\boldsymbol{x}_F^{(k)}$ can be generated as

$$\boldsymbol{x}_F^{(k.0)} = \boldsymbol{s}(\boldsymbol{F}^{(k)}) \tag{19}$$

The benefits of using the inverse surrogate, apart from the fact that the inverse model directly produces the antenna parameter vector without the need of launching the optimization process, are similar to those pertinent to the response feature approach. In particular, the relationship between the performance figures and geometry parameters is less nonlinear than the relationship between the parameters and antenna outputs. This is illustrated in Fig. 3, showing the reflection response of the ring slot antenna considered in Section IV at the design $\boldsymbol{x}^{(1)}$ optimized for the frequency $f_0 = 4.5$ GHz and implemented on the substrate of relative permittivity $\varepsilon_r = 3.5$, which is the objective vector $\boldsymbol{F}^{(1)}$. The initial design $\boldsymbol{x}^{(2.0)}$ obtained using the inverse surrogate for $\boldsymbol{F}^{(2)} = [f_0\ \varepsilon_r]^T$ with $f_0 = 4.0$ GHz and $\varepsilon_r = 4.4$ is of good quality, whereas the design obtained by optimizing the forward linear model of the form of (11) is considerably worse in terms of allocating the operating frequency of the antenna. This was despite the fact that a reasonable value of the search radius (normally not available beforehand) was used when optimizing the forward model. For the objective vector $\boldsymbol{F}^{(3)} = [f_0\ \varepsilon_r]^T$ with $f_0 = 3.0$ GHz and $\varepsilon_r = 3.0$ (i.e., farther away from $\boldsymbol{F}^{(1)}$), the benefits of using the inverse surrogate are even more pronounced. Although the prediction of the inverse model is not perfect, it is significantly better than that of the forward one.

Another benefit of the inverse surrogate is that it allows for a rapid correction of the design (at the cost of just one EM simulation) if necessary. A correction can be realized as follows. Let $\boldsymbol{F}_{extr}^{(k)}$ be the actual objective vector extracted from EM simulated antenna responses at the design $\boldsymbol{x}_F^{(k.0)}$ obtained as in (19). The prediction error $\Delta\boldsymbol{F}$ is then calculated as the difference between the target and the actual objective vectors, i.e.,

$$\Delta\boldsymbol{F} = \boldsymbol{F}^{(k)} - \boldsymbol{F}_{extr}^{(k)} \tag{20}$$

The corrected design can be then obtained as

$$\boldsymbol{x}_{F.corr}^{(k.0)} = \boldsymbol{s}(\boldsymbol{F}^{(k)} + \Delta\boldsymbol{F}) \tag{21}$$

In other words, the correction (21) accommodates the prediction error and improves the design by reevaluating the inverse surrogate upon including $\Delta\boldsymbol{F}$. The source of the error is a nonlinear dependence between $\boldsymbol{F}$ and $\boldsymbol{x}$, which is merely approximated by the linear inverse surrogate (18). The effect of correction has been illustrated in Fig. 4.

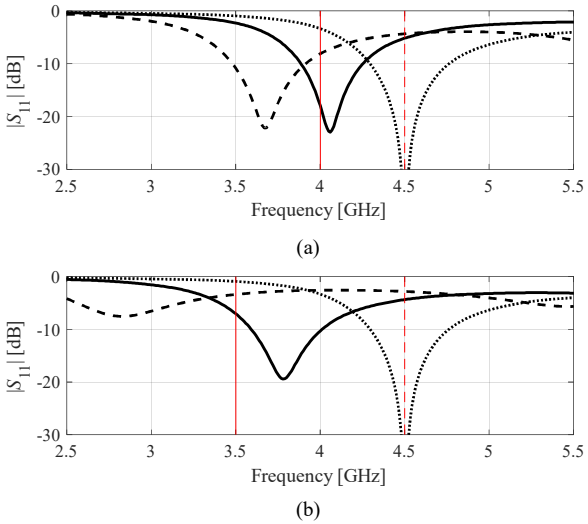

(a)

(b)

Fig. 3. Inverse surrogate for initial design generation shown for a ring-slot antenna considered in Section IV. Reflection response at the center design $\boldsymbol{x}^{(1)} = U^*(\boldsymbol{F}^{(1)})$ (····), design prediction obtained using the inverse surrogate (18) (—) and the forward model (11) (- - -): (a) design $\boldsymbol{x}^{(2)}$ corresponding to the objective vector $\boldsymbol{F}^{(2)} = [f_0\ \varepsilon_r]^T$ with $f_0 = 4.0$ GHz and $\varepsilon_r = 4.4$, and (b) design $\boldsymbol{x}^{(3)}$ corresponding to the objective vector $\boldsymbol{F}^{(3)} = [f_0\ \varepsilon_r]^T$ with $f_0 = 3.5$ GHz and $\varepsilon_r = 3.0$. Note that prediction of the inverse model is significantly more reliable. The vertical lines denote operating frequencies at the center design (- - -), and the target (—).

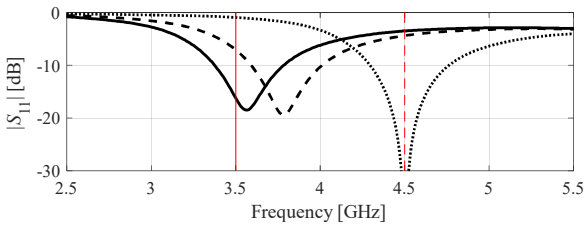

Fig. 4. Design correction (21) illustrated for an exemplary ring slot antenna of Section IV. Reflection response at the center design $\boldsymbol{x}^{(1)} = U^*(\boldsymbol{F}^{(1)})$ (····), design prediction obtained using the inverse surrogate (18) (- - -) and the corrected design (21) (—). The data has been shown for the objective vector $\boldsymbol{F}^{(3)} = [f_0\ \varepsilon_r]^T$ with $f_0 = 3.5$ GHz and $\varepsilon_r = 3.0$.

B. Feature-Based Parameter Tuning

Given the initial point $\boldsymbol{x}_F^{(k.0)}$, the optimization process will be continued using the trust-region (TR) gradient based algorithm similar (12). Whenever possible, the original formulation of the design problem (1) will be replaced by the feature-based formulation (cf. Section II.*B*). Thus, the optimum database design $\boldsymbol{x}_F^{(k)}$ will be obtained through a series of approximations $\boldsymbol{x}_F^{(k.i)}$ generated as

$$\boldsymbol{x}_F^{(k.i+1)} = \arg\min_{\boldsymbol{x};\,-\boldsymbol{d}^{(i)} \le \boldsymbol{x}-\boldsymbol{x}_F^{(k.i)} \le \boldsymbol{d}^{(i)}} U_F^{(i)}(\boldsymbol{x}, \boldsymbol{F}^{(k)}) \tag{22}$$

$i = 1, 2, \ldots$, where $U_F^{(i)}$ is the feature-based objective function evaluated using the first-order Taylor expansion model $\boldsymbol{L}_F^{(k.i)}$ of $\boldsymbol{R}$ of the form

$$\boldsymbol{L}_F^{(k.i+1)} = \boldsymbol{R}(\boldsymbol{x}_F^{(k.i)}) + \boldsymbol{J}(\boldsymbol{x}_F^{(k.i)}) \cdot (\boldsymbol{x} - \boldsymbol{x}_F^{(k.i)}) \tag{23}$$

The Jacobian $\boldsymbol{J}$ is estimated using finite differentiation in the first iteration and updated using the Broyden formula [56] afterwards. The trust region is defined through its lower and upper bounds $\boldsymbol{x}^{(i)} - \boldsymbol{d}^{(i)} \le \boldsymbol{x} \le \boldsymbol{x}^{(i)} + \boldsymbol{d}^{(i)}$, where the inequalities are understood component-wise. The size vector $\boldsymbol{d}^{(i)}$ is adjusted using the standard TR rules [55]. Using an interval-type of TR region eliminates the need for variable scaling, which is especially important when the parameter ranges vary significantly (e.g., transmission line lengths versus line gaps, etc.).

C. Optimization Framework

Here, we outline the operation of the entire optimization framework proposed in this paper. The framework utilizes the components described in Sections II as well as the routines formulated in Sections III.*A* and III.*B* as the building blocks. The input parameters of the procedure are the following:

- EM simulation model $\boldsymbol{R}$ of the antenna under optimization;
- Definition of the response features $\boldsymbol{p}$ for the model $\boldsymbol{R}$ (cf. Section II.*B*);
- Objective vectors $\boldsymbol{F}^{(k)} \in F$, $k = 1, \ldots, p$, for which the database designs are to be acquired;
- Assessment function $f_a(\boldsymbol{x},\boldsymbol{F}) = f_a(\boldsymbol{p}(\boldsymbol{x}),\boldsymbol{F})$ (cf. Section II.*B*) and the acceptance threshold $f_{a.\max}$ for f_a (to be used to either accept or reject the initial design produced by the inverse surrogate);
- Maximum number of objective vector relaxations $j_{\max}$;
- Maximum acceptable value of the objective function $U_{F.\max}$.

The role of the assessment function and the acceptance threshold is to determine whether the quality of the design produced at the particular stage of the optimization process is sufficient to move on to the next stage. If the assessment is negative, typically, a new (corrected) design is produced, or the design specifications are temporarily relaxed (at most $j_{\max}$ times) to enable approaching the original target in smaller steps. The design obtained through local tuning is considered acceptable if the corresponding objective function value does not exceed $U_{F.\max}$.

The operating flow of the proposed optimization procedure can be summarized as follows:

1. Assign $\boldsymbol{F}^{(1)}$ as the objective vector closest to $\boldsymbol{F}_c = p^{-1}\sum_k \boldsymbol{F}^{(k)}$;
2. Obtain the first design $\boldsymbol{x}_F^{(1)} = U^*(\boldsymbol{F}^{(1)})$ using direct search (typically, using feature-based optimization [39]);
3. Estimate the inverse sensitivity matrix $\boldsymbol{J}^x(\boldsymbol{F}^{(1)})$ as in Section II.*C*;
4. Using $\boldsymbol{J}^x(\boldsymbol{F}^{(1)})$, set up the inverse surrogate $\boldsymbol{s}(\boldsymbol{F})$ (18);
5. Set the design counter to $k = 2$;
6. Using the inverse surrogate $\boldsymbol{s}(\boldsymbol{F})$, find the initial design $\boldsymbol{x}_F^{(k.0)} = \boldsymbol{s}(\boldsymbol{F}^{(k)})$;
7. **If** $f_a(\boldsymbol{x}_F^{(k.0)}) \le f_{a.\max}$,
   Go to Step 15;
   else
   Calculate the error $\Delta\boldsymbol{F} = \boldsymbol{F}^{(k)} - \boldsymbol{F}_{extr}^{(k)}$ (20); find the corrected design $\boldsymbol{x}_{F.corr}^{(k.0)} = \boldsymbol{s}(\boldsymbol{F}^{(k)} + \Delta\boldsymbol{F})$ (21), and, if $f_a(\boldsymbol{x}_{F.corr}^{(k.0)}) < f_a(\boldsymbol{x}_F^{(k.0)})$, set $\boldsymbol{x}_F^{(k.0)} = \boldsymbol{x}_{F.corr}^{(k.0)}$;
   end
8. **If** $f_a(\boldsymbol{x}_F^{(k.0)}) \le f_{a.\max}$,
   Go to Step 15;
   end
9. Set $j = 1$ (local counter);
10. Extract the actual objective vector $\boldsymbol{F}_{extr}$ at the design $\boldsymbol{x}_F^{(k.0)}$; calculate the updating factor $t = \min\left\{1, \dfrac{f_{a.\max}}{\| \boldsymbol{F}^{(k)} - \boldsymbol{F}_{extr} \|}\right\}$;
11. Update the objective vector as $\boldsymbol{F}_{tmp}^{(k)} = \boldsymbol{F}_{extr} + t(\boldsymbol{F}^{(k)} - \boldsymbol{F}_{extr})$;
12. Update the initial design as $\boldsymbol{x}_F^{(k.0)} = \arg\min_{\boldsymbol{x}} U_F(\boldsymbol{x}, \boldsymbol{F}_{tmp}^{(k)})$; the problem is solved using TR gradient search (cf. Section III.*B*);
13. Set $j = j + 1$;
14. **If** ($f_a(\boldsymbol{x}_F^{(k.0)}) \le f_{a.\max}$ AND $t = 1$) OR $j > j_{\max}$ (use $\boldsymbol{F}_{tmp}^{(k)}$ in place of $\boldsymbol{F}^{(k)}$ when evaluating f_a),
   Set $\boldsymbol{x}_F^{(k)} = \boldsymbol{x}_F^{(k.0)}$ and go to Step 16;
   else
   Go to Step 10;
   end
15. Find $\boldsymbol{x}_F^{(k)}$ as $\boldsymbol{x}_F^{(k)} = \arg\min_{\boldsymbol{x}} U_F(\boldsymbol{x}, \boldsymbol{F}^{(k)})$; the problem is solved using the TR gradient search (cf. Section III.*B*);
16. Store the design $\boldsymbol{x}_F^{(k)}$ along with the corresponding actual value of the objective vector $\boldsymbol{F}_{extr}^{(k)}$. Set $k = k + 1$;
17. If $k \le p$ go to 6;
18. END.

The first four steps of the procedure (Steps 1-4) are executed to prepare the inverse surrogate (18) as discussed in Section III.*A*. Steps 5 through 17 are performed in a loop to generate all p database designs. The initial design generated in Step 6 is either accepted based on the assessment function value, in which case it undergoes further tuning (Step 15), or it is rejected and the correction is made (cf. (20), (21)). If the corrected initial design is not accepted, the auxiliary tuning process is launched for relaxed objective vector calculated based on the performance of the current design (Steps 10 and 11). In Step 12, the TR algorithm is initially executed with the Broyden updates, which requires just one EM antenna analysis per algorithm iteration. In the case of failure (i.e., $U_F(\boldsymbol{x}_F^{(k.0)}) > U_{F.\max}$), another round is launched using full finite-differentiation updates. The series of auxiliary tuning runs is terminated once the relaxed specifications become sufficiently close to the original ones or the maximum number of these is exceeded.

The overall assumption of the procedure is that the required database designs can be found for the antenna at hand, i.e., it is possible to optimize the structure for all objective vectors $\boldsymbol{F}^{(k)}$,

and that the local tuning is sufficient if the initial design is sufficiently close to the target. If this assumption is not satisfied, the procedure would still operate but some of the designs may not adhere to the original targets. The operation of the procedure is also explained using the flow diagram presented in Fig. 5.

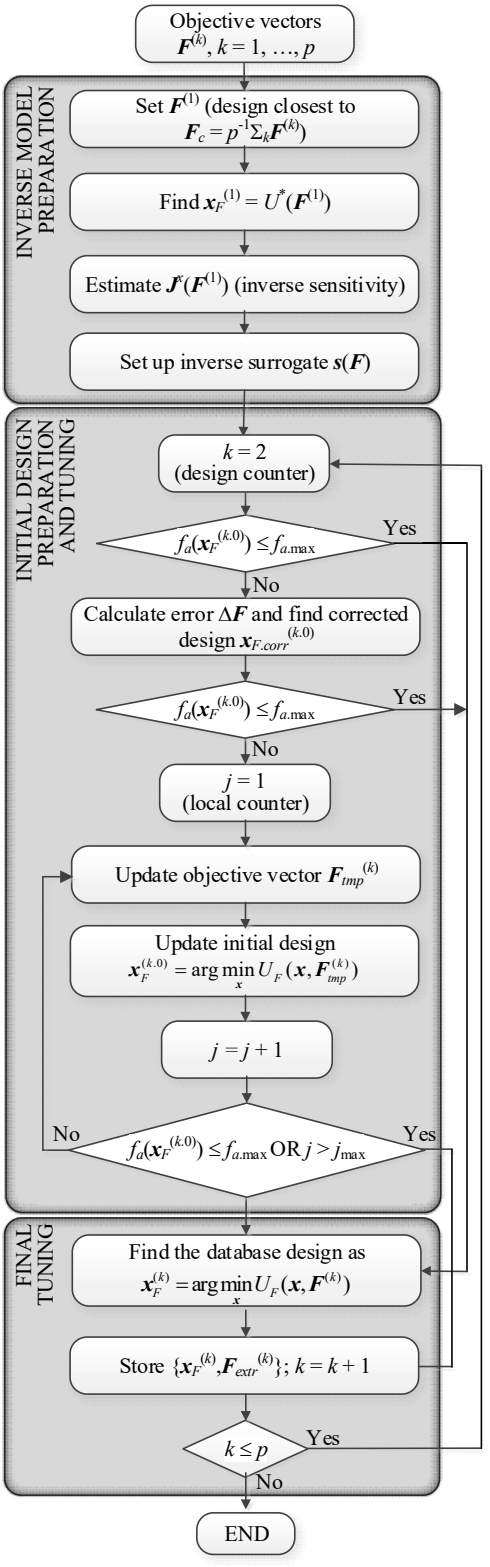

Fig. 5. Flow diagram of the proposed optimization procedure for generating database designs.

IV. Demonstration Case Studies

The proposed optimization framework is demonstrated in this section using three examples of microstrip antennas, specifically, a dual-band uniplanar dipole antenna and a ring-slot antenna considered in [43] as verification cases for the nested kriging framework, as well as a quasi-Yagi antenna that will be used to illustrate the warm-start optimization procedure [48]. This allows us to put our methodology in the right application context, as performance-driven modelling and rapid dimension scaling are representative applications that require generation of the database designs. In these cases, the algorithm is employed for the assumed objective space, relevant to the modelling/design tasks at hand. For comparison, the same designs are obtained using a traditional method, which is by executing independent optimization runs with initial designs produced through experience-driven parameter sweeping. Afterwards, the designs are applied as reference points for setting up the nested kriging surrogate model or the surrogate-assisted warm-start optimization framework. This allows us to emphasize the computational benefits offered by the presented approach, where fast rendering of the reference points enables considerable savings in terms of the overall cost of surrogate model setup.

A. Case I: Dual-Band Uniplanar Dipole Antenna

Consider a dual-band uniplanar dipole antenna shown in Fig. 6 [57], implemented on RO4350 substrate (ε_r = 3.5, h = 0.76 mm). The design variables are $\boldsymbol{x} = [l_1\ l_2\ l_3\ w_1\ w_2\ w_3]^T$, other parameters are fixed (see [43] for details). The computational model model $\boldsymbol{R}$ is simulated in CST Microwave Studio (~100,000 cells; simulation time 1 minute). In [43], the task was to render a surrogate model of the antenna input characteristics, which was supposed to be valid within the objective space defined by the following ranges of the operating frequencies: 2.0 GHz $\le f_1 \le$ 3.0 GHz for the lower band, and 4.0 GHz $\le f_2 \le$ 5.5 GHz for the upper band. The modeling framework referred to as nested kriging, requires a certain number of so-called reference designs $\boldsymbol{x}^{(j)}$, $j = 1, \ldots, p$. These are employed to set up an auxiliary first-level model, subsequently utilized to define the constrained domain of the surrogate model. In [43], the reference designs corresponded to the following pairs of f_1 and f_2 (frequencies in GHz): [2.0 4.0], [2.6 4.0], [3.0 4.0], [2.3 4.5], [2.8 4.7], [2.2 5.0], [2.7 5.3], [2.0 5.5], [2.4 5.5], and [3.0 5.5].

As described in Section III, the pair $[2.2\ 5.0]^T$ was selected as $\boldsymbol{F}^{(1)}$ (the vector closest to $\boldsymbol{F}_c = p^{-1}\Sigma_k \boldsymbol{F}^{(k)}$). The design $\boldsymbol{x}_F^{(1)} = U^*(\boldsymbol{F}^{(1)})$ was found using feature-based optimization [39] at the cost of sixty EM analyses of the antenna. In the next stage, the inverse sensitivity $\boldsymbol{J}^x$ was estimated using the methodology of Section II.*C*. The CPU cost of this stage was 33 antenna simulations. The remaining database designs were obtained using Steps 5 through 18 of the algorithm of Section III.*C*, using the assessment function of the form of (8) and the acceptance threshold $f_{a.\max}$ = 0.3. It turns out that this verification case was not difficult for the proposed procedure, in particular, the initial designs generated by the inverse surrogate satisfied the condition $f_a(\boldsymbol{x}_F^{(k.0)}) \le f_{a.\max}$ for all $k = 2, \ldots, p$. Thus, neither the initial design correction (Step 7) nor objective relaxation (Steps 10-12) were

This article has been accepted for publication in a future issue of this journal, but has not been fully edited. Content may change prior to final publication. Citation information: DOI 10.1109/TAP.2021.3074632, IEEE Transactions on Antennas and Propagation

necessary. The final tuning was performed using the trust-region gradient search (Step 15) at the level of response features. The average computational cost of finding the database points is 26 antenna simulations (per design). The overall cost including all aforementioned contributors (antenna optimization for $\boldsymbol{F}^{(1)}$, estimating inverse sensitivity, and identification of the remaining designs) is only 264 EM analyses of the antenna. For comparison, the same database designs were found using a conventional approach, i.e., through direct gradient-based optimization, starting from the design $\boldsymbol{x}_F^{(1)}$ in each case. Even though feature-based approach was used, the total cost amounts to 930 EM analyses. Optimization involving minimax formulation (cf. (2)) was even more expensive as it required a certain amount of parameter sweeping in order to generate reasonable starting points for some of the database designs. The total cost of it was 1201 EM simulations of the antenna. Table I shows the summary of the optimization cost for conventional and proposed approaches. Figure 7 shows the antenna responses at the selected database designs indicating good alignment of the resonances with the target operating frequencies.

As mentioned before, the database designs were used as the reference points for setting up the nested kriging surrogate model of the antenna of Fig. 6. The details of the technique can be found in [43]. In short, the nested kriging employs two kriging interpolation metamodels. The first-level (inverse) model $\boldsymbol{s}_I$ is constructed using $\{\boldsymbol{F}^{(j)},\boldsymbol{x}^{(j)}\}, j = 1, \ldots, p$, to approximate the region containing designs that are optimum with respect to all vectors $\boldsymbol{F}$ within the considered objective space. The image of the objective space through $\boldsymbol{s}_I$ is extended to establish the domain of the final, second-level surrogate. As indicated in [43], confining the model domain this way has profound effects on the predictive power of the surrogate and allows us to render reliable models over broad ranges of geometry parameters and operating conditions of the antenna.

Figure 8 shows the responses of the nested kriging surrogate (obtained using N = 400 training samples) as well as the EM simulated antenna characteristics at the selected test locations. The average relative RMS error of the model is only 2.6%. Table II summarizes the computational cost of setting up the model for two scenarios concerning reference point acquisition: conventional (feature-based) and the method proposed in this work. It should also be mentioned that the traditional kriging surrogate constructed for the same antenna without domain confinement exhibits the error of almost 10% when using 400 training samples, which is four time higher than that of the nested kriging. The technique proposed in this work results in 50 percent savings over conventional reference design acquisition when using feature-based formulation. The savings over reference design generation using minimax formulation are even higher (59 percent).

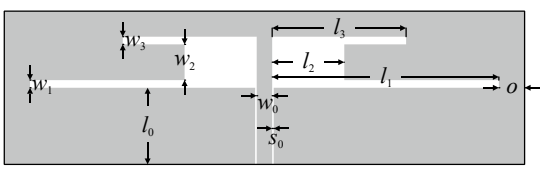

Fig. 6. Dual-band uniplanar dipole antenna: geometry [57].

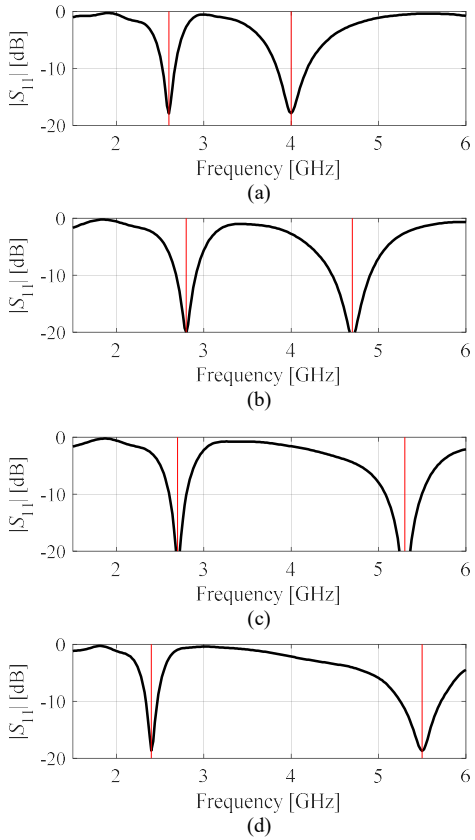

Fig. 7. Dual-band dipole antenna: reflection response at the selected database designs found using the proposed optimization framework (frequencies in GHz): (a) [f_1 f_2] = [2.6 4.0], (b) [f_1 f_2] = [2.8 4.7], (c) [f_1 f_2] = [2.7 5.5], (d) [f_1 f_2] = [2.4 5.5]. Target operating frequencies marked using vertical lines.

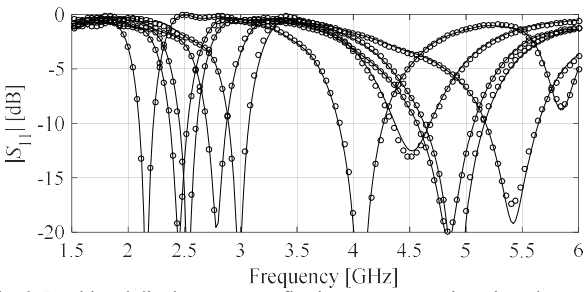

Fig. 8. Dual-band dipole antenna: reflection response at the selected test designs for the nested kriging surrogate constructed using 400 training samples (o). EM simulation results at the same test locations are marked using the solid line (—).

TABLE I DUAL-BAND ANTENNA: OPTIMIZATION COST OF DATABASE DESIGN GENERATION

Optimization technique	Computational cost[&]	
	Total[*]	Per design
Conventional (minimax)[#]	1201	120.1
Conventional (feature-based)[$]	930	93.0
Proposed in this work	264	26.4

[&]Computational cost expressed in number of EM analyses of the antenna structure under optimization.
[#]Gradient-based optimization using minimax formulation (cf. (2)) with starting points adjusted using auxiliary parameter sweeping.
[$]Feature-based optimization (cf. (7)) with starting point adjusted using auxiliary parameter sweeping.
[*]The database set consists of 10 designs.

This article has been accepted for publication in a future issue of this journal, but has not been fully edited. Content may change prior to final publication. Citation information: DOI 10.1109/TAP.2021.3074632, IEEE Transactions on Antennas and Propagation

TABLE II DUAL-BAND ANTENNA: COMPUTATIONAL COST OF CONSTRUCTING THE NESTED KRIGING SURROGATE

Computational cost component[#]	Method of generating reference designs	
	Conventional (feature-based formulation)	This work
Reference design acquisition	930	264
Training data acquisition[$]	400	400
Total cost	1330	664

[#]Cost expressed in the number of EM analyses of the antenna structure.
[$]EM simulations necessary to acquire training data samples for second-level surrogate construction.

B. Case II: Ring-Slot Antenna

Consider a slot antenna shown in Fig. 9 [58], implemented on a 0.76-mm-thick substrate. The geometry parameters are $\boldsymbol{x} = [l_f\ l_d\ w_d\ r\ s\ s_d\ o\ g]^T$. The substrate permittivity ε_r is one of the objective space components. The feed line width w_f is calculated for a given ε_r to ensure 50 ohm input impedance. The EM model is implemented in CST (~300,000 cells, simulation 90 s). The modeling task considered in [43] was to construct a surrogate model of the antenna input characteristics, valid over the objective space defined by the following ranges of the operating frequency f and the substrate permittivity ε_r: 2.5 GHz $\le f \le$ 6.5 GHz, and $2.0 \le \varepsilon_r \le 5.0$. Similarly as before, the surrogate is to be constructed using nested kriging. The reference designs are selected to correspond to the following pairs of f and ε_r (frequency in GHz): $[f, \varepsilon_r]$ = [2.5 2.0], [4.5 2.0], [6.5 2.0], [2.5 3.5], [4.0 3.5], [5.0 3.5], [6.5 3.5], [2.5 5.0], [4.5 5.0], and [6.5 5.0].

The objective vector $[5.0\ 3.5]^T$ was selected as $\boldsymbol{F}^{(1)}$ (the vector closest to $\boldsymbol{F}_c = p^{-1}\sum_k \boldsymbol{F}^{(k)}$). Feature-based optimization [39] was employed to find $\boldsymbol{x}_F^{(1)} = U^*(\boldsymbol{F}^{(1)})$ at the cost of 85 EM analyses of the antenna. The inverse sensitivity $\boldsymbol{J}^x$ was estimated as in Section II.*C* at the cost of 45 antenna simulations. The remaining designs were found using the algorithm of Section III.*C*, using the assessment function of the form of (8) and the acceptance threshold $f_{a.\max} = 0.5$. This problem is more challenging from the optimization perspective, and, in some cases, the correction of the initial design (Step 7) and objective relaxation was necessary. The final tuning was performed using the trust-region gradient search with the feature-based formulation.

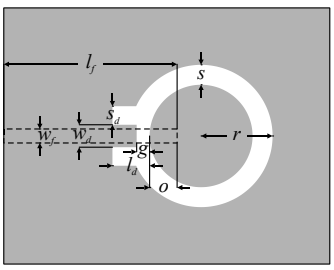

Fig. 9. Ring-slot antenna: geometry (feeding line shown using dashed lines) [58].

The average cost of identifying the database points is only 37 antenna simulations (per design). The overall cost is 368 EM analyses. As a benchmark, the same database designs were found using a conventional approach with both the minimax and feature-based formulations. The corresponding costs are gathered in Table III. Note that the proposed approach enables considerable computational savings: 64 percent over conventional method with minimax formulation and 57 percent over conventional method with feature-based formulation. Figure 10 shows the antenna responses at the selected database designs.

The database designs were applied to construct the nested kriging surrogate of the antenna of Fig. 9. A brief outline of the modeling procedure has been provided in Section IV.*A*. found in [43]. Figure 11 shows the responses of the surrogate (obtained using N = 400 training samples) along with the EM simulated antenna characteristics at the selected test locations. The average relative RMS error of the model is only 3.1%. Table IV summarizes the computational cost of setting up the model for two scenarios concerning reference point acquisition: conventional (feature-based) and the method proposed in this work. The proposed technique enables 40 percent savings over conventional reference design acquisition when using feature-based formulation. The savings over reference design generation using minimax formulation are as high as 46 percent.

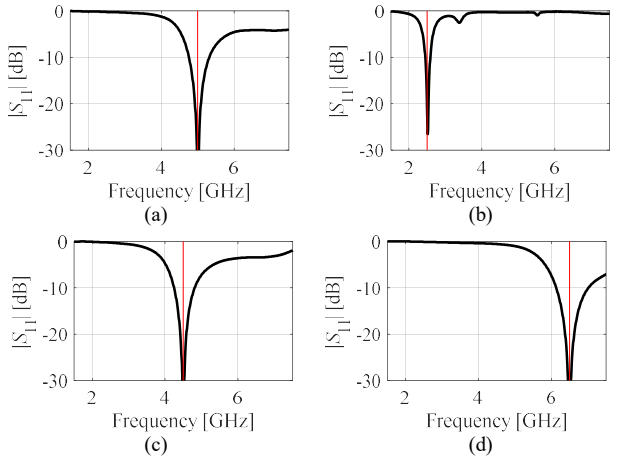

Fig. 10. Ring-slot antenna: reflection response at the selected database designs found using the proposed optimization framework (frequencies in GHz): (a) $[f\ \varepsilon_r]$ = [5.0 3.5], (b) $[f\ \varepsilon_r]$ = [2.5 5.0], (c) $[f\ \varepsilon_r]$ = [4.5 2.0], (d) $[f\ \varepsilon_r]$ = [6.5 3.5].

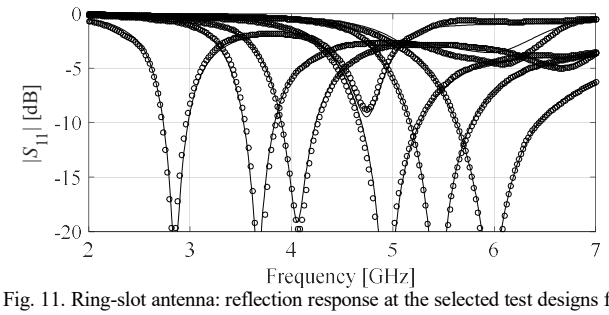

Fig. 11. Ring-slot antenna: reflection response at the selected test designs for the nested kriging surrogate constructed using 400 training samples (o). EM simulation results at the same test locations are marked using the solid line (—).

TABLE III RING-SLOT ANTENNA: OPTIMIZATION COST OF DATABASE DESIGN GENERATION

Optimization technique	Computational cost[&]	
	Total[*]	Per design
Conventional (minimax)[#]	1012	101.2
Conventional (feature-based)[$]	864	86.4
Proposed in this work	368	36.8

[&]Computational cost expressed in number of EM analyses of the antenna structure under optimization.
[#]Gradient-based optimization using minimax formulation (cf. (2)) with starting points adjusted using auxiliary parameter sweeping.
[$]Feature-based optimization (cf. (7)) with starting point adjusted using auxiliary parameter sweeping.
[*]The database set consists of 10 designs.

TABLE IV RING-SLOT ANTENNA: COMPUTATIONAL COST OF CONSTRUCTING THE NESTED KRIGING SURROGATE

Computational cost component[#]	Method of generating reference designs	
	Conventional (feature-based formulation)	This work
Reference design acquisition	864	368
Training data acquisition[$]	400	400
Total cost	1264	768

[#]Cost expressed in the number of EM analyses of the antenna structure.
[$]EM simulations necessary to acquire training data samples for second-level surrogate construction

It should be reiterated that the traditional kriging surrogate constructed for this antenna without domain confinement exhibits the error of over 25% even when using 800 training samples [43], which makes it unsuitable for design purposes. This indicates that the initial cost of rendering the reference design is unavoidable to construct a reliable model. Still, the proposed approach allows us to reduce it in a considerable manner.

C. Case III: Quasi-Yagi Antenna

Our last demonstration case is a quasi-Yagi antenna with a parabolic reflector (Fig. 12) [59], implemented on a 1.5-mm-thick substrate. The EM model is simulated in CST. The design variables are $\boldsymbol{x} = [W\ L\ L_m\ L_p\ S_d\ S_r\ W_2\ W_a\ W_d\ g]^T$ (all dimensions in mm). The parameter W_1 (feed line width) is calculated for a given substrate permittivity ε_r to ensure 50-ohm input impedance.

The antenna of Fig. 12 will be utilized as a verification case for the warm-start optimization procedure [48], where a set of database designs was used to construct two kriging metamodels: (i) an inverse model (similar to $\boldsymbol{s}_I$ of the nested kriging) employed to generate the initial design for further tuning, and (ii) a forward model of antenna response sensitivities. The latter allowed for jump-starting the gradient-based tuning process, executed with the trust-region framework and the Broyden update [56].

The specific design task was to optimize the antenna for a given center frequency f_0 and to ensure 8-percent fractional bandwidth (symmetric w.r.t. f_0). This was to be done for the assumed substrate permittivity ε_r. Another goal was to maximize the average realized gain within the same bandwidth (cf. (5)). The objective space is defined by the following ranges: 2.5 GHz $\le f_0 \le$ 5.0 GHz and $2.5 \le \varepsilon_r \le 4.5$. The database designs correspond to the pairs $[f_0\ \varepsilon_r]$ (frequencies in GHz): [2.5 4.5], [3.5 4.5], [5.0 4.5], [2.5 2.5], [5.0 2.5], [3.5 2.5], [4.5 3.5], and [3.0 3.5].

In this case, although $\boldsymbol{F}_c = p^{-1}\sum_k \boldsymbol{F}^{(k)}) = [3.75\ 3.5]^T$, the vector $[3.5\ 4.5]^T$ is selected as $\boldsymbol{F}^{(1)}$, which is because the sensitivity of optimum antenna parameters with respect to the substrate permittivity is significantly lower than with respect to the operating frequency. The design $\boldsymbol{x}_F^{(1)} = U^*(\boldsymbol{F}^{(1)})$ was found at the cost of 105 EM analyses of the antenna. The cost of estimating the inverse sensitivity $\boldsymbol{J}^x$ was 39 antenna simulations. The remaining designs were found using the algorithm of Section III.*C*, using the assessment function (9) and the acceptance threshold $f_{a.\max} = 0.3$. From the point of view of generating the database design, this problem is the most challenging out of the three considered in this work because the response feature technique cannot be directly applied. Consequently, in most cases, both the initial design correction (Step 7) and objective relaxation was required. The average cost of identifying the database points is around 43 antenna simulations (per design) with the overall cost equal to 342 EM. The cost of finding the database designs using a conventional approach was 1899 EM analyses (cf. Table V). Thus, the computational savings due to the proposed methodology are as high as 82 percent. The antenna responses at the selected database designs have been shown in Fig. 13.

As mentioned before, the database designs are used to implement the warm-start optimization framework [48]. It is validated by optimizing the antenna for the selected objective vectors (the ensembles of the antenna operating frequency and substrate permittivity). The selected results have been shown in Fig. 14. Clearly, reducing the set up cost of the framework by a factor over eighty percent, as achieved by means of accelerated generation of the database designs, is highly desirable from a practical design perspective.

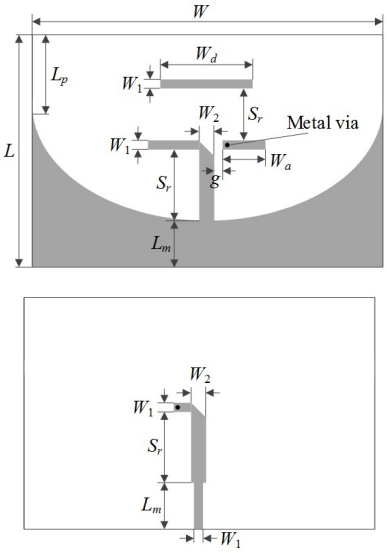

Fig. 12. Quasi-Yagi antenna: geometry [59]: top layer (top), bottom layer (bottom).

This article has been accepted for publication in a future issue of this journal, but has not been fully edited. Content may change prior to final publication. Citation information: DOI 10.1109/TAP.2021.3074632, IEEE Transactions on Antennas and Propagation

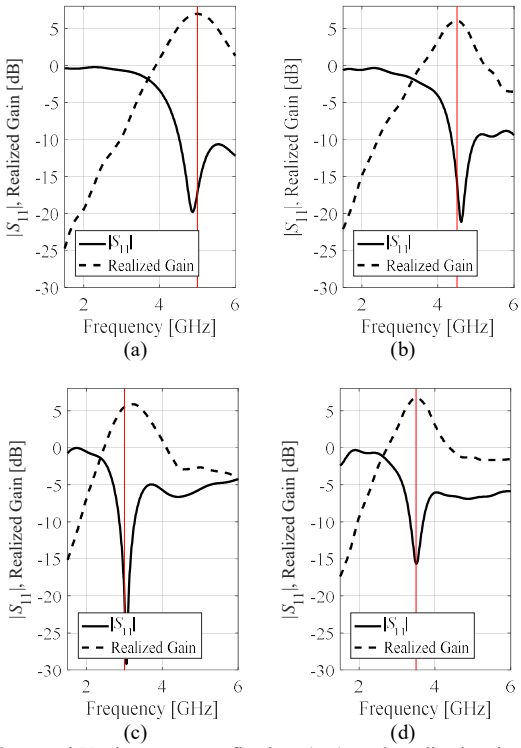

Fig. 13. Quasi-Yagi antenna: reflection (top) and realized gain (bottom) characteristics at the selected database designs found using the proposed optimization framework (frequencies in GHz): (a) $[f_0\ \varepsilon_r] = [5.0\ 4.5]$, (b) $[f_0\ \varepsilon_r] = [4.5\ 3.5]$, (c) $[f_0\ \varepsilon_r] = [3.0\ 3.5]$, (d) $[f_0\ \varepsilon_r] = [3.5\ 4.5]$.

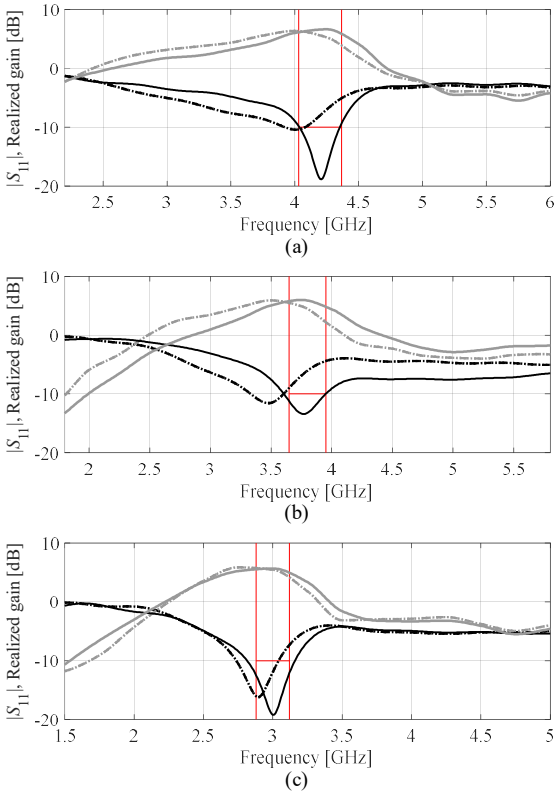

Fig. 14. Quasi-Yagi antenna: reflection (black) and realized gain (gray) responses at the initial (····) and the optimized (—) designs corresponding to the target objective vectors: (a) $f_0 = 4.2$ GHz, $\varepsilon_r = 2.5$, (b) $f_0 = 3.8$ GHz, $\varepsilon_r = 3.5$, and (c) $f_0 = 3.0$ GHz, $\varepsilon_r = 4.4$. The initial designs are generated by the inverse model constructed using the database designs (cf. [57]).

TABLE V QUASI-YAGI ANTENNA: OPTIMIZATION COST OF DATABASE DESIGN GENERATION

Optimization technique	Computational cost[&]	
	Total[*]	Per design
Conventional[#]	1899	237.4
Proposed in this work	342	42.7

[&]Computational cost expressed in number of EM analyses of the antenna structure under optimization.
[#]Gradient-based optimization using formulation (5) with starting points adjusted using auxiliary parameter sweeping.
[*]The database set consists of 8 designs.

V. CONCLUSION

The paper presented an optimization framework for expedited acquisition of database designs, i.e., optimized sets of antenna parameters corresponding to selected values of performance figures (e.g., an operating frequency) or material parameters (e.g., substrate permittivity). The ensembles of such designs are important for performance-driven modelling procedures, construction of inverse surrogates, or rapid re-design (dimension scaling) of antenna structures. At the same time, carrying out multiple optimization runs for different performance requirements is a challenging endeavour, which entails considerable computational expenses. The methodology proposed in this work alleviates these difficulties and enables accelerated acquisition of the database designs by means of inverse sensitivities and inverse surrogate modelling as well as feature-based tuning procedure.

Our framework has been comprehensively validated using three antenna structures. Superiority over conventional optimization procedures involving experience-driven initial design appointment has been conclusively demonstrated with the speedup from 57 to 82 percent with the average of over 70 percent for a range of considered benchmark set. Another benefit of the presented approach is to enable design automation, specifically, generation of the entire set of database designs without user supervision. This may not be possible for a traditional approach, especially when the designs are to be generated for broad ranges of antenna operating conditions. The proposed technique can be useful for expedited construction of database designs for constrained modeling procedures, building the inverse surrogates, as well as implementing frameworks for rapid re-design and dimension scaling of antenna structures.

A comment should be made concerning the scalability of the presented method. Based on the presented evidence of three test cases of increasing dimensionality (six, eight, and ten parameters) as well as average costs of databased design acquisition (26, 37, and 43 EM analyses per design), it seems that the dependence of the computational expenses and the number of parameters is weaker than linear. This is to be expected because of the fact that the computational costs are mainly determined by the dimensionality of the objective space, which is normally low (one, two, or three), which is another benefit of the incorporation of inverse modeling techniques.

The employment of EM simulation tools to antenna design, in particular, EM-driven optimization, is widespread and still growing. The authors believe that the methodology presented

in this work may become a stimulus for the development of yet better and more reliable optimization methods that would alleviate the difficulties related to high cost of massive simulations, especially within scenarios involving the execution of repetitive optimization runs or similar tasks.

ACKNOWLEDGEMENT

The authors would like to thank Dassault Systemes, France, for making CST Microwave Studio available.

REFERENCES

[1] D.I.L. de Villiers, I. Couckuyt, and T. Dhaene, "Multi-objective optimization of reflector antennas using kriging and probability of improvement," *Int. Symp. Ant. Prop.*, pp. 985-986, San Diego, USA, 2017.

[2] S. An, S. Yang and O.A. Mohammed, "A Kriging-assisted light beam search method for multi-objective electromagnetic inverse problems," *IEEE Trans. Magn.*, vol. 54, no. 3, pp. 1-4, 2018.

[3] B. Liu, M.O. Akinsolu, N. Ali, and R. Abd-Alhameed, "Efficient global optimization of microwave antennas based on a parallel surrogate model-assisted evolutionary algorithm," *IET Microwaves Ant. Prop.*, vol. 13, no. 2, pp. 149-155, 2019.

[4] A.K.S.O. Hassan, A.S. Etman, and E.A. Soliman, "Optimization of a novel nano antenna with two radiation modes using kriging surrogate models," *IEEE J. Photonics*, vol. 10, no. 4, Art. Seq. No. 4800807, 2018.

[5] D.R. Prado, J.A. Lopez-Fernandez, M. Arrebola, and G. Goussetis, "Support vector regression to accelerate design and crosspolar optimization of shaped-beam reflectarray antennas for space applications," *IEEE Trans. Ant. Prop.*, vol. 67, no. 3, pp. 1659-1668, 2018.

[6] E. Hassan, D. Noreland, R. Augustine, E. Wadbro, and M. Berggren, "Topology optimization of planar antennas for wideband near-field coupling," *IEEE Trans. Ant. Prop.*, vol. 63, no. 9, pp. 4208-4213, 2015.

[7] J. Wang, X.S. Yang, and B.Z. Wang, "Efficient gradient-based optimization of pixel antenna with large-scale connections," *IET Microwaves Ant. Prop.*, vol. 12, no. 3, pp. 385-389, 2018.

[8] J. Du and C. Roblin, "Statistical modeling of disturbed antennas based on the polynomial chaos expansion," *IEEE Ant. Wireless Prop. Lett.*, vol. 16, p. 1843-1847, 2017.

[9] M. Rossi, A. Dierck, H. Rogier, and D. Vande Ginste, "A stochastic framework for the variability analysis of textile antennas," *IEEE Trans. Ant. Prop.*, vol. 62, no. 16, pp. 6510-6514, 2014.

[10] J.S. Ochoa and A.C. Cangellaris, "Random-space dimensionality reduction for expedient yield estimation of passive microwave structures," *IEEE Trans. Microwave Theory Techn.*, vol. 61, no. 12, pp. 4313-4321, 2013.

[11] J.A. Easum, J. Nagar, P.L. Werner, and D.H. Werner, „Efficient multiobjective antenna optimization with tolerance analysis through the use of surrogate models," *IEEE Trans. Ant. Prop.*, vol. 66, no. 12, pp. 6706-6715, 2018.

[12] J. Dong, W. Qin, and M. Wang, "Fast multi-objective optimization of multi-parameter antenna structures based on improved BPNN surrogate model," *IEEE Access*, vol. 7, pp. 77692-77701, 2019.

[13] S. Koziel and A.T. Sigurdsson, "Multi-fidelity EM simulations and constrained surrogate modeling for low-cost multi-objective design optimization of antennas," *IET Microwaves Ant. Prop.*, vol. 12, no. 13, pp. 2025-2029, 2018.

[14] J. Zhang, C. Zhang, F. Feng, W. Zhang, J. Ma, and Q.J. Zhang, "Polynomial chaos-based approach to yield-driven EM optimization," *IEEE Trans. Microwave Theory Tech.*, vol. 66, no. 7, pp. 3186-3199, 2018.

[15] A. Kouassi, N. Nguyen-Trong, T. Kaufmann, S. Lallechere, P. Bonnet, and C. Fumeaux, "Reliability-aware optimization of a wideband antenna," *IEEE Trans. Ant. Prop.*, vol. 64, no. 2, pp. 450-460, 2016.

[16] D. Gorissen, K. Crombecq, I. Couckuyt, T. Dhaene, and P. Demeester, „A surrogate modeling and adaptive sampling toolbox for computer based design," *J. Machine Learning Research*, vol. 11, pp. 2051-2055, 2010.

[17] S. Marelli and B. Sudret, „UQLab: a framework for uncertainty quantification in Matlab," in *The 2nd Int. Conf. on Vulnerability and Risk Analysis and Management (ICVRAM 2014)*, University of London, UK, July 13-15, pp. 2554-2563, 2014.

[18] Matlab, ver. R2018b, The Mathworks Inc., Natick, MA, USA, 2018.

[19] J.L. Chávez-Hurtado and J.E. Rayas-Sánchez, "Polynomial-based surrogate modeling of RF and microwave circuits in frequency domain exploiting the multinomial theorem," *IEEE Trans. Microwave Theory Tech.*, vol. 64, no. 12, pp. 4371-4381, 2016.

[20] N.V. Queipo, R.T. Haftka, W. Shyy, T. Goel, R. Vaidynathan, and P.K. Tucker, "Surrogate-based analysis and optimization," *Progress in Aerospace Sciences*, vol. 41, no. 1, pp. 1-28, 2005.

[21] P. Barmuta, F. Ferranti, G.P. Gibiino, A. Lewandowski, and D.M.M.P. Schreurs, "Compact behavioral models of nonlinear active devices using response surface methodology," *IEEE Trans. Microwave Theory and Tech.,* vol. 63, no. 1, pp. 56-64, 2015.

[22] J.E. Rayas-Sanchez and V. Gutierrez-Ayala, "EM-based statistical analysis and yield estimation using linear-input and neural-output space mapping," *IEEE MTT-S Int. Microwave Symp. Digest (IMS)*, pp. 1597-1600, 2006.

[23] J. Cai, J. King, C. Yu, J. Liu, and L. Sun, "Support vector regression-based behavioral modeling technique for RF power transistors," *IEEE Microwave and Wireless Comp. Lett.,* vol. 28, no. 5, pp. 428-430, 2018.

[24] A. Petrocchi, A. Kaintura, G. Avolio, D. Spina, T. Dhaene, A. Raffo, and D.M.P.-P. Schreurs, „Measurement uncertainty propagation in transistor model parameters via polynomial chaos expansion," *IEEE Microwave Wireless Comp. Lett.*, vol. 27, no. 6, pp. 572-574, 2017.

[25] G. Taskin, H. Kaya, and L. Bruzzone, „Feature selection based on high dimensional model representation for hypersprectral images," *IEEE Trans. Image Proc.*, vol. 26,no. 6, pp. 2918-2928, 2017.

[26] A.C. Yücel, H. Bağcı, and E. Michielssen, "An ME-PC enhanced HDMR method for efficient statistical analysis of multiconductor transmission line networks," *IEEE Trans. Comp. Packaging and Manufacturing Techn.*, vol .5, no. 5, pp. 685-696, 2015.

[27] X. Li, "Finding deterministic solution from underdetermined equation: large-scale performance modeling of analog/RF circuits," *IEEE Trans. on Computer-Aided Design of Integrated Circuits and Systems* (*TCAD*), vol. 29, no. 11, pp. 1661-1668, 2010.

[28] R. Hu, V. Monebhurrun, R. Himeno, H. Yokota, and F. Costen, „An adaptive least angle regression method for uncertainty quantification in FDTD computation," *IEEE Trans. Ant. Prop.*, vol. 66, no. 12, pp. 7188-7197, 2018.

[29] M.C. Kennedy and A. O'Hagan, "Predicting the output from complex computer code when fast approximations are available", *Biometrika,* vol. 87, pp. 1-13, 2000.

[30] J.P. Jacobs and S. Koziel, "Two-stage framework for efficient Gaussian process modeling of antenna input characteristics," *IEEE Trans. Antennas Prop.*, vol. 62, no. 2, pp. 706-713, 2014.

[31] F. Wang, P. Cachecho, W. Zhang, S. Sun, X. Li, R. Kanj, and C. Gu, "Bayesian model fusion: large-scale performance modeling of analog and mixed-signal circuits by reusing early-stage data," *IEEE Trans. on Computer-Aided Design of Integrated Circuits and Systems (TCAD)*, vol. 35, no. 8, pp. 1255-1268, 2016.

[32] S. Koziel, J.W. Bandler, and K. Madsen, "Theoretical justification of space-mapping-based modeling utilizing a data base and on-demand parameter extraction," *IEEE Trans. Microwave Theory Tech*., vol. 54, no. 12, pp. 4316-4322, Dec. 2006.

[33] S. Koziel and L. Leifsson, *Simulation-driven design by knowledge-based response correction techniques*, Springer, New York, 2016.

[34] J.W. Bandler, Q.S. Cheng, S.A. Dakroury, A.S. Mohamed, M.H. Bakr, K. Madsen, and J. Sondergaard, "Space mapping: the state of the art," *IEEE Trans. Microwave Theory Tech.*, vol. 52, no. 1, pp. 337-361, Jan. 2004.

[35] F. Feng, J. Zhang, W. Zhang, Z. Zhao, J. Jin, and Q.J. Zhang, „Coarse- and fine-mesh space mapping for EM optimization incorporating mesh deformation," *IEEE Microwave Wireless Comp. Lett.*, vol. 29, no. 8, pp. 510-512, 2019.

[36] J.E. Rayas-Sanchez, „Power in simplicity with ASM: tracing the aggressive space mapping algorithm over two decades of development and engineering applications," *IEEE Microwave Mag.*, vol. 17, no. 4, pp. 64-76, 2016.

[37] D. Echeverria and P.W. Hemker, "Space mapping and defect correction," *CMAM, Int. Math. J. Comp. Methods in Applied Math.,* vol. 5, no. 2, pp. 107-136, 2005.

[38] S. Koziel and S.D. Unnsteinsson "Expedited design closure of antennas by means of trust-region-based adaptive response scaling," *IEEE Antennas Wireless Prop. Lett.*, vol. 17, no. 6, pp. 1099-1103, 2018.
[39] S. Koziel, "Fast simulation-driven antenna design using response-feature surrogates," *Int. J. RF & Microwave CAE*, vol. 25, no. 5, pp. 394-402, 2015.
[40] S. Koziel, "Low-cost data-driven surrogate modeling of antenna structures by constrained sampling," *IEEE Antennas Wireless Prop. Lett.*, vol. 16, pp. 461-464, 2017.
[41] S. Koziel and A.T. Sigurdsson, "Triangulation-based constrained surrogate modeling of antennas," *IEEE Trans. Ant. Prop.*, vol. 66, no. 8, pp. 4170-4179, 2018.
[42] S. Koziel and A. Pietrenko-Dabrowska, "Reduced-cost surrogate modeling of compact microwave components by two-level kriging interpolation," *Eng. Opt.*, vol. 52, no. 6, pp. 960-972, 2019.
[43] S. Koziel and A. Pietrenko-Dabrowska, "Performance-based nested surrogate modeling of antenna input characteristics," *IEEE Trans. Ant. Prop.*, vol. 67, no. 5, pp. 2904-2912, 2019.
[44] A. Pietrenko-Dabrowska and S. Koziel, "Antenna modeling using variable-fidelity EM simulations and constrained co-kriging," *IEEE Access*, vol. 8, no. 1, pp. 91048-91056, 2020.
[45] A. Pietrenko-Dabrowska and S. Koziel, "Reliable surrogate modeling of antenna input characteristics by means of domain confinement and principal components," *Electronics*, vol. 9, no. 5, pp. 1-16, 2020.
[46] A. Pietrenko-Dabrowska, S. Koziel, and M. Al-Hasan, „Cost-efficient bi-layer modeling of antenna input characteristics using gradient kriging surrogates," *IEEE Access*, 2020.
[47] S. Ulaganathan, I. Couckuyt, T. Dhaene, E. Laermans, and J. Degroote, "On the use of gradients in Kriging surrogate models," *Proc Winter Simulation Conf. 2014*, Savanah, GA, pp. 2692–2701, 2014.
[48] A. Pietrenko-Dabrowska and S. Koziel, „Accelerated design optimization of miniaturized microwave passives by design reusing and kriging interpolation surrogates," *AEU Int. J. Electronics Comm.*, vol. 118, 2020.
[49] U. Ullah, S. Koziel, and I.B. Mabrouk, "Rapid re-design and bandwidth/size trade-offs for compact wideband circular polarization antennas using inverse surrogates and fast EM-based parameter tuning," *IEEE Trans. Ant. Prop.*, vol. 68, no. 1, pp. 81-89, 2019.
[50] M. Caenepeel, F. Ferranti, and Y. Rolain, "Efficient and automated generation of multidimensional design curves for coupled-resonator filters using system identification and metamodels," *Int. Conf. Synthesis, Modeling, Analysis Sim. Methods App. Circuit Design*, Lisbon, 2016.
[51] G. Gosal, E. Almajali, D. McNamara, and M. Yagoub, "Transmitarray antenna design using forward and inverse neural network modeling," *IEEE Ant. Wireless Prop. Lett.*, vol. 15, pp. 1483-1486, 2016.
[52] S. Koziel and A. Pietrenko-Dabrowska, "Rapid optimization of compact microwave passives using kriging surrogates and iterative correction," *IEEE Access*, vol. 8, pp. 53587-53594, 2020.
[53] S. Koziel and J.W. Bandler, "Rapid yield estimation and optimization of microwave structures exploiting feature-based statistical analysis," *IEEE Trans. Microwave Theory Tech.*, vol. 63, no., 1, pp. 107-114, 2015.
[54] S. Koziel and A. Pietrenko-Dabrowska, "Expedited feature-based quasi-global optimization of multi-band antennas with Jacobian variability tracking," *IEEE Access*, vol. 8, pp. 83907-83915, 2020.
[55] A.R. Conn, N.I.M. Gould, and P.L. Toint, *Trust Region Methods*, MPS-SIAM Series on Optimization, 2000.
[56] C.G. Broyden, "A class of methods for solving nonlinear simultaneous equations," *Math. Comp.*, vol. 19, pp. 577-593, 1965.
[57] Y.-C. Chen, S.-Y. Chen, and P. Hsu, "Dual-band slot dipole antenna fed by a coplanar waveguide," *IEEE Int. Symp. Ant. Prop.*, pp. 3589-3592, 2006.
[58] C. Y. D. Sim, M. H. Chang, and B. Y. Chen, "Microstrip-fed ring slotantenna design with wideband harmonic suppression,"IEEE Trans. An-tennas Propag., vol. 62, no. 9, pp. 4828–4832, 2014.
[59] Z. Hua, G. Haichuan, L. Hongmei, L. Beijia, L. Guanjun, and W. Qun, "A novel high-gain quasi-Yagi antenna with a parabolic reflector," *Int. Symp. Ant. Prop. (ISAP)*, Hobart, Australia, 2015.

SLAWOMIR KOZIEL received the M.Sc. and Ph.D. degrees in electronic engineering from Gdansk University of Technology, Poland, in 1995 and 2000, respectively. He also received the M.Sc. degrees in theoretical physics and in mathematics, in 2000 and 2002, respectively, as well as the PhD in mathematics in 2003, from the University of Gdansk, Poland. He is currently a Professor with the Department of Engineering, Reykjavik University, Iceland. His research interests include CAD and modeling of microwave and antenna structures, simulation-driven design, surrogate-based optimization, space mapping, circuit theory, analog signal processing, evolutionary computation and numerical analysis.

ANNA PIETRENKO-DABROWSKA received the M.Sc. and Ph.D. degrees in electronic engineering from Gdansk University of Technology, Poland, in 1998 and 2007, respectively. Currently, she is an Associate Professor with Gdansk University of Technology, Poland. Her research interests include simulation-driven design, design optimization, control theory, modeling of microwave and antenna structures, numerical analysis.